# Abrupt Climate Oscillations During the Last Deglaciation in Central North America

**Zicheng Yu* and Ulrich Eicher**

**Evidence from stable isotopes and a variety of proxies from two Ontario lakes demonstrate that many of the late glacial–to–early Holocene events that are well known from the North Atlantic seaboard, such as the Gerzensee-Killarney Oscillation (also known as the Intra-Allerød Cold Period), Younger Dryas, and Preboreal Oscillation, also occurred in central North America. These results thus imply that climatic forcing acted in the same manner in both regions and that atmospheric circulation played an important role in the propagation of these events.**

The transition from the last glacial maximum to the present interglacial (Holocene) has great importance in understanding how Earth's climate system can abruptly switch from one state to another. The most detailed records of this transition—the late glacial period—are from the North Atlantic region, which appears to have acted as either a trigger or an amplifier of late glacial climate events. This transition [~13,000 to 9000 $^{14}$C years before the present (yr B.P.)] was characterized by several broad-scale climatic oscillations in the North Atlantic region (*1–6*). Isotopic records from Europe (*4, 7, 8*) and Greenland ice cores (*2, 3*) reveal a late glacial climate sequence in which the warm Bølling-Allerød (BOA) was followed by the cold Younger Dryas (YD) at ~11,000 to 10,000 $^{14}$C yr B.P. and then by the warm Holocene. In continental North America, however, climate proxy data provide mixed and limited evidence for these climate oscillations (*9*), and this sequence was not seen in isotopic records (*10*). Establishing the geographic extent, sequence, and magnitude of these climate oscillations is essential for understanding the mechanisms and causes of abrupt short-term climatic changes.

Here we describe several sedimentary records from two small lakes (Fig. 1), which show the late glacial and early Holocene climate changes. The two sites from separate basins eliminate local hydrology as the cause of observed changes. The basins are predominately situated in Ordovician and Silurian dolomites covered by thin glacial deposits. Three cores of sediment from Crawford Lake (43°28′N, 79°57′W) and one from Twiss Marl Pond (informal name; 43°27′N, 79°57′W) were analyzed for carbonate stable isotopes ($\delta^{18}$O and $\delta^{13}$C), lithology, elemental geochemistry, pollen, plant macrofossils, and freshwater gastropods. The $\delta^{18}$O values from bulk marl and mollusk shells were used as proxy for temperature (*11*). Other proxy data were used to infer lake and watershed conditions during climatic changes (Fig. 2) (*12*). Chronology was controlled by four AMS $^{14}$C dates on terrestrial plant macrofossils and by correlation with dated regional pollen sequences (*13*).

The $^{18}$O/$^{16}$O ratios ($\delta^{18}$O) in authigenic lake carbonates are a proxy of continental climate and depend on the isotopic composition of lake water and on water temperature. The isotopic fractionation between calcite and water varies by −0.24 per mil (‰) per degree celsius of temperature (*14*). A strong positive link between $\delta^{18}$O in atmospheric precipitation and mean annual surface temperature exists in the high and mid-latitude regions; the average coefficient is about 0.6‰ per degree celsius (*15*). The combination of these two factors and the assumption that water temperature closely tracks air temperature lead to an estimate of a coefficient of 0.36‰ per degree celsius between $\delta^{18}$O in carbonate and air temperature. In the late glacial and early Holocene, the climate in the Great Lakes region resembled that of a high-latitude region. A strong temperature gradient likely prevailed immediately south of the continental ice sheets (*16*). The climatic regime during that time may have imposed a strong link between $\delta^{18}$O and temperature, so the variation of temperatures along this strong gradient might be sensitively reflected in $\delta^{18}$O values of atmospheric precipitation.

The $\delta^{18}$O results from mollusk shells (Fig. 2A) and from *Chara* encrustations and bulk marl (*17, 18*) at Twiss Marl Pond show a negative shift of 1.3‰ at 10,920 $^{14}$C yr B.P. (at 490 cm) and a positive shift of up to 2‰ at ~10,000 $^{14}$C yr B.P. (at 390 cm). The more negative intervening interval indicates a cold period corresponding with the YD event. A minor negative excursion of 0.4‰ at 9600 $^{14}$C yr B.P. (at 370 to 380 cm) may correlate with the Preboreal Oscillation (PB) (*1–5, 7*). This minor oscillation is also indicated by the recurrence of *Picea* pollen at Twiss Marl Pond and more clearly at Crawford Lake and by a distinct minerogenic layer (Fig. 2B). Before the YD interval, another slight negative excursion of $\delta^{18}$O at 500 to 510 cm in mollusk shells may correlate with the Gerzensee Oscillation (G) in central Europe (*7, 4*), the Killarney Oscillation (K) in Atlantic Canada (*6*), and the Intra-Allerød Cold Period (IACP) in Greenland (*1–3*). It is also indicated by a peak for elemental Al.

The $\delta^{18}$O profile of core SC (Fig. 2C) from the shallow basin at Crawford Lake shows the BOA warming at ~12,500 $^{14}$C yr B.P. (minimum 1‰ positive shift in $\delta^{18}$O from 378.5 to 374 cm); the BOA warm period from ~12,300 to 11,000 $^{14}$C yr B.P. (from 374 to 361 cm); a pre-YD cooling event, corresponding with G/K/IACP oscillations,

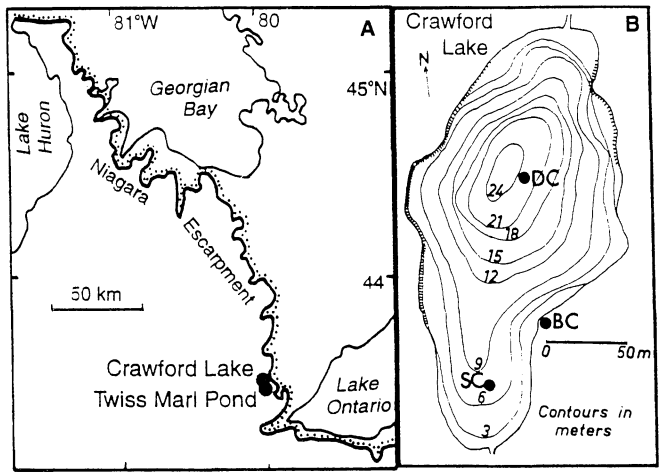


**Fig. 1.** Map showing locations of Crawford Lake and Twiss Marl Pond at the edge of Ontario's Niagara Escarpment, Canada (**A**), and coring locations (DC, SC, and BC) at Crawford Lake (**B**).

Z. C. Yu, Department of Botany, University of Toronto, Toronto, Ontario M5S 3B2, Canada, and Centre for Biodiversity and Conservation Biology; Royal Ontario Museum, Toronto, Ontario M5S 2C6, Canada. U. Eicher, Climate and Environmental Physics, Physics Institute, University of Bern, CH-3012 Bern, Switzerland.

*To whom correspondence should be addressed at the Canadian Forest Service, 5320 122 Street, Edmonton, Alberta T6H 3S5, Canada. E-mail: zyu@nrcan.gc.ca

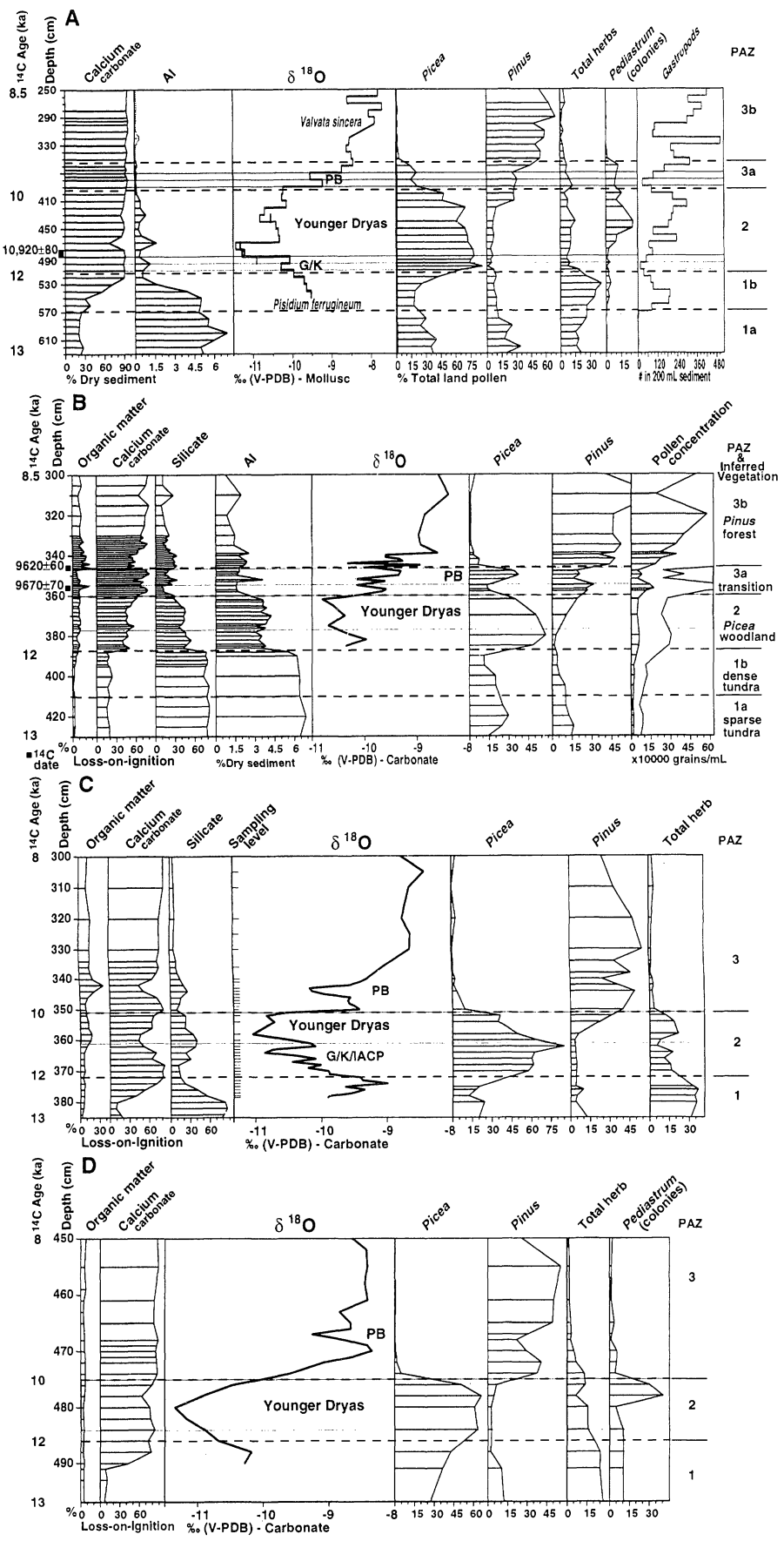


shortly before 11,000 $^{14}$C yr B.P. (at 364 cm: ~0.8‰ negative excursion); the YD cold period from 11,000 to 10,000 $^{14}$C yr B.P. (from 361 to 350 cm: 1.5‰ negative excursion); the Holocene warming at 10,000 yr B.P. (at 351 cm: ~1.5‰ positive shift); and the PB at 9650 $^{14}$C yr B.P. (at 344 cm: 0.4‰ negative excursion). Cores DC (Fig. 2B) and BC (Fig. 2D) at Crawford Lake show similar patterns but with a thinner record and lower temporal resolution.

These observed patterns cannot be attributed to local hydrological effects, because (i) similar patterns are seen at the two sites, (ii) dissolution of dolomite bedrock (with a $\delta^{18}$O value of −6.46‰) as suggested by elemental geochemistry and lithology analysis (Fig. 2) (*18*) cannot account for the observed patterns, and (iii) the $\delta^{18}$O records from both sites correlate well with the $\delta^{18}$O records from Greenland ice cores (Fig. 3) and central European lake sediments. For the carbonate $\delta^{18}$O–air temperature correlation of 0.36‰ per degree celsius, the 1‰ decrease in $\delta^{18}$O at the beginning of the YD event could imply a 3°C decrease in mean annual air temperature, and the 2‰ increase at the beginning of the Holocene could imply a 6°C increase. This relation may, however, not be valid for long-term climatic change. For example, we have no independent data to evaluate the evaporative enrichment of $\delta^{18}$O (*19*). The $\delta^{18}$O values suggest that temperature or precipitation (or both) may have fluctuated during the YD event, as also seen in European (*7*) and Greenland isotopic records (Fig. 3). The YD event appears to have been cold at the beginning and slightly warmer in the middle. The variations during the YD interval are also indicated by elemental concentrations and sediment composition at two study sites. These new records are comparable in sequence and relative magnitude with records from ice cores (*2, 3*), and marine (*1*) and European lacustrine sediments (*4, 7, 8*).

At Twiss Marl Pond and Crawford Lake, the YD cooling is indicated by a negative excursion in $\delta^{18}$O values together with a persistence of and slight increase in shrub and herb pollen, a slight decrease of pollen concentration, decreased carbonate, and in-

**Fig. 2.** Combined diagrams of proxy climate data recorded in the late glacial and early Holocene sediments at Twiss Marl Pond (**A**) and in core DC (**B**), core SC (**C**), and core BC (**D**) at Crawford Lake. PB, Preboreal Oscillation; G/K/IACP, Gerzensee (*7*), Killarney (*6*), and Intra-Allerød Cold Period (*1*); V-PDB, Vienna Pee Dee belemnite; PAZ, pollen assemblage zones. At Twiss Marl Pond, the $\delta^{18}$O was measured on shells of two mollusk species, *Pisidium ferrugineum* (lower thick line) and *Valvata sincera* (upper thin line). A more detailed discussion is given elsewhere (*18*). All data will be available at www.ngdc.noaa.gov/paleo/paleo.html.

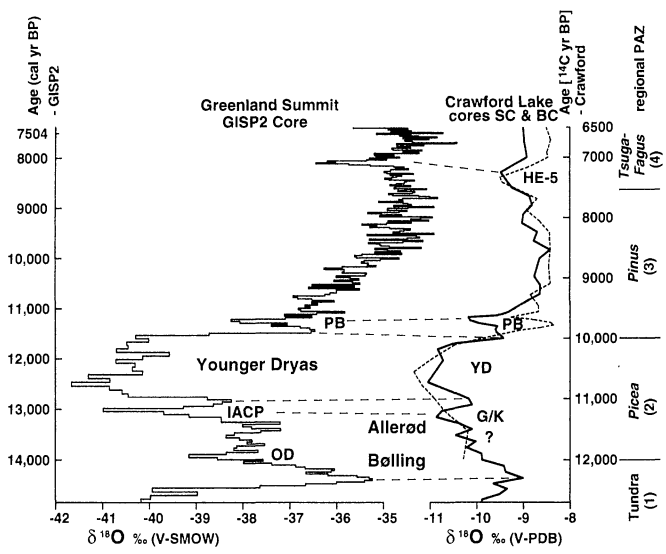


**Fig. 3.** Correlation of Greenland ice core [Greenland Ice Sheet Project 2 (GISP2)] $\delta^{18}O$ (left bar-curve) (*2*) and Crawford Lake (core SC, heavy curve; core BC, dashed curve) carbonate $\delta^{18}O$ profiles on calendar- and $^{14}C$-year time scales, respectively. The calendar ages from GISP2 are from annual ice layer counting, and the $^{14}C$ ages from Crawford Lake are based on AMS $^{14}C$ dates at the two study sites and on correlation with the dated regional pollen sequence (*13*). At Crawford Lake, the sequence of climatic oscillations includes the BOA warming, G/K/IACP, YD, PB, and HE-5 (*22*), and possibly OD (Older Dryas). HE-5 here is dated at approximately 7500 $^{14}C$ yr B.P., based on the major *Pinus*–to–*Tsuga-Fagus* pollen transition and is equivalent to the cooling event at Greenland Summit at 8200 calendar years B.P. (*20*). All these oscillations recorded at Crawford Lake are about one-third to one-half the amplitude of the Greenland record, and PB and HE-5 are half the amplitude of the YD and of G/K/IACP at both locations.

creased erosion-derived elements, all of which suggest more openings in forests and accelerated soil erosion under a cold climate. The lack of strong upland vegetational evidence for the YD at the two study sites is attributed to an insensitive response of the nonecotonal vegetation at that time (*18*). A decrease in calcite precipitation or an increase in eroded minerogenic matter during the YD cold interval has been recorded at marl lakes in Switzerland (*4*).

Two cores (SC and BC) from Crawford Lake (Fig. 3) also show evidence for the short-term cooling event at approximately 8200 calendar yr B.P. (~7500 $^{14}C$ yr B.P.). The $\delta^{18}O$ values drop by ~0.8‰ then, or about half the magnitude of the YD cooling. This prominent Holocene climatic event is widespread and has left a global record (*20, 21*). This event and the PB have been termed Holocene Events 5 and 8 (HE-5 and HE-8), respectively, from the North Atlantic marine sediments (*22*). At Crawford Lake after ~6500 $^{14}C$ yr B.P., the $\delta^{18}O$ profiles (*23*) are no longer correlative with Greenland isotopic records, which suggests that the climatic regime appears to have changed and that climatic change occurred more frequently on a regional basis.

The sequence and relative magnitude of late glacial–early Holocene climatic changes recorded at Crawford Lake and Twiss Marl Pond match in detail the records from the North Atlantic region and indicate that these oscillations are probably an expression of broad climatic changes. Our data show that, in addition to the YD, other minor oscillations (PB and G/K/IACP) affected the climate beyond the North Atlantic region. The close match of the $\delta^{18}O$ records at the two sites presented in this study and at other sites in the North Atlantic region indicates that the climatic forcing acted in the same manner in both the North Atlantic region and interior North America and that the climatic signals were probably carried through the atmosphere over the Northern Hemisphere.

### References and Notes


1. S. J. Lehman and L. D. Keigwin, *Nature* **356**, 757 (1992).
2. P. M. Grootes, M. Stuiver, J. W. C. White, S. Johnsen, J. Jouzel, *ibid.* **366**, 552 (1993).
3. S. J. Johnsen *et al.*, *ibid.* **359**, 311 (1992); W. Dansgaard *et al.*, *ibid.* **364**, 218 (1993).
4. A. F. Lotter, U. Eicher, H. J. B. Birks, U. Siegenthaler, *J. Quat. Sci.* **7**, 187 (1992).
5. S. Björck *et al.*, *Science* **274**, 1155 (1996).
6. A. J. Levesque, F. E. Mayle, I. R. Walker, L. C. Cwynar, *Nature* **361**, 623 (1993).
7. U. Eicher and U. Siegenthaler, *Boreas* **5**, 109 (1976); U. Eicher, *Mitt. Naturforsch. Ges. Bern N.F.* **37**, 65 (1980); U. Siegenthaler, U. Eicher, H. Oeschger, *Ann. Glaciol.* **5**, 149 (1984); U. Eicher, *Geogr. Helv.* **2**, 99 (1987).
8. T. Goslar *et al.*, *Nature* **377**, 414 (1995); K. Ahlberg, E. Almgren, H. E. Wright Jr., E. Ito, S. Hobbie, *Boreas* **25**, 257 (1996).
9. *Picea* pollen recurrence from the southern Great Lakes region is interpreted as climate cooling, correlative to the YD interval [L. C. K. Shane, *Boreas* **16**, 1 (1987); H. E. Wright Jr., *Quat. Sci. Rev.* **8**, 295 (1989)]. Fossil insects from the Great Lakes region, however, indicate a stable climate condition without a major climate amelioration around the onset of the Holocene at ~11,000 to 9000 $^{14}C$ yr B.P. [S. A. Elias, K. H. Anderson, J. T. Andrews, *J. Quat. Sci.* **11**, 417 (1996)].
10. M. Stuiver, *Science* **162**, 994 (1968); *J. Geophys. Res.* **75**, 5247 (1970); P. Fritz, A. V. Morgan, U. Eicher, J. H. McAndrews, *Palaeogeogr. Palaeoclimatol. Palaeoecol.* **58**, 183 (1987); but see A. Shemesh and D. Peteet, *Geophys. Res. Lett.* **25**, 1935 (1998). Isotopic records from the Great Lakes are difficult to interpret in terms of climate changes because of the complex hydrologic budget [P. Fritz, T. W. Anderson, C. F. M. Lewis, *Science* **190**, 267 (1975); C. F. M. Lewis and T. W. Anderson, *Clim. Dyn.* **6**, 241 (1992); D. K. Rea *et al.*, *Geology* **22**, 1059 (1994)].
11. The analytical procedure and methodology used are similar to that used for marine sediment [J. M. McCrea, *J. Chem. Phys.* **18**, 849 (1950)]. Each sample of 5 to 40 mg of carbonate was reacted with 95% phosphoric acid ($H_3PO_4$) at a constant temperature of 50°C for 1 hour to produce $CO_2$. The $CO_2$ was then analyzed for its $^{18}O/^{16}O$ and $^{13}C/^{12}C$ ratios with a mass spectrometer (Finnigan MAT 250) at the University of Bern (*19*). The results are presented as conventional delta notation ($\delta$), which is defined as $[(R_{sample} - R_{standard})/R_{standard}] \times 1000$ [where $R$ is the absolute ratio of $^{18}O/^{16}O$ or $^{13}C/^{12}C$, and the Vienna-PDB (Pee Dee belemnite) is the standard]. The analytical precision is ±0.02‰ for both $\delta^{18}O$ and $\delta^{13}C$. The authigenic calcite is the dominant carbonate in bulk samples, as confirmed at selected levels by calcite and dolomite determinations, petrographic microscope analysis, and almost identical isotope values of *Chara* encrustations and corresponding bulk samples (*18*).
12. The organic matter and carbonate contents of sediments were estimated by loss-on-ignition analysis. Elemental concentrations were determined by neutron activation analysis of bulk sediment. Four cores at two sites show a sediment sequence from clay to clayey marl to marl (Fig. 2). See (*18*) for detail on lithology and elemental stratigraphy. Pollen stratigraphy indicates a change in vegetation from an *Alnus*, Cyperaceae, *Salix* sparse tundra (subzone 1a) through *Salix*, Cyperaceae, *Artemisia* dense tundra (subzone 1b) and *Picea* woodland (zone 2) to *Pinus* forest (zone 3) (Fig. 2). The vegetation reconstruction was substantiated by plant macrofossils from two sites (*18*).
13. Two accelerator mass spectrometry (AMS) $^{14}C$ dates from 355 to 357 cm and 345 to 347 cm of core DC at Crawford Lake bracket a mineral-rich sediment band, corresponding with the PB as indicated by the *Picea* pollen recurrence (Fig. 2B). The dates of 9670 ± 70 (CAMS-16061) and 9620 ± 60 yr B.P. (CAMS-16062) are statistically indistinguishable because of a $^{14}C$ plateau around 9600 $^{14}C$ yr B.P. [B. Becker, B. Kromer, P. Trimborn, *Nature* **353**, 647 (1991); I. Hajdas *et al.*, *Clim. Dyn.* **9**, 107 (1993)]. The AMS date of 10,920 ± 80 $^{14}C$ yr B.P. (TO-5505) from Twiss Marl Pond (Fig. 2A) is used for the lower boundary of the YD interval, as correlated with the negative shift in $\delta^{18}O$ within the *Picea* pollen zone. Other dates are based on local deglaciation history and regional pollen correlation. The base of the records was tentatively assigned an age of 13,000 $^{14}C$ yr B.P. based on deglaciation history [P. J. Barnett, *Can. J. Earth Sci.* **16**, 568 (1979)]. The shrub/herb-*Picea* pollen transition (zone 1/2 at the boundary) was about 12,000 $^{14}C$ yr B.P., estimated from nearby dated sites [R. J. Mott and L. D. Farley-Gill, *Can. J. Bot.* **15**, 1101 (1978); J. Terasmae and H. L. Matthews, *Can. J. Earth Sci.* **17**, 1087 (1980)]. The age of the *Picea*-*Pinus* pollen transition (zone 2/3) was close to 10,000 $^{14}C$ yr B.P., as interpolated and extrapolated from Crawford Lake and other sites [K. D. Bennett, *Can. J. Bot.* **65**, 1792 (1987); J. M. Szeicz and G. M. MacDonald, *ibid.* **69**, 1507 (1991)]. The *Pinus*–to–*Tsuga-Fagus* pollen transition (zone 3/4) has an age of close to 7500 $^{14}C$ yr B.P. [J. H. McAndrews, in *Quaternary Paleoclimate*, W. C. Mahaney, Ed. (Geo Abstracts, Norwich, England, 1981), pp. 319–333].
14. I. Friedman and J. R. O'Neil, in *Data of Geochemistry*, I. Friedman and J. R. O'Neil, Eds. [U.S. Geological Survey (USGS) Professional Paper 440-KK, KK1-12, USGS, Washington, DC, 1977].
15. W. Dansgaard, *Tellus* **16**, 436 (1964); K. Rozanski, L. Araguas-Araguas, R. Gonfiantini, *Science* **258**, 981 (1992).
16. COHMAP Members, *Science* **241**, 1043 (1988); T. Webb III *et al.*, in *Global Climates Since the Last Glacial Maximum*. H. E. Wright Jr. *et al.*, Eds. (Univ. of Minnesota Press, Minneapolis, MN, 1993), pp. 514–535; A. J. Levesque, L. C. Cwynar, I. R. Walker, *Nature* **385**, 423 (1997).
17. Z. C. Yu and U. Eicher, data not shown.
18. Z. C. Yu, thesis, University of Toronto (1997).
19. U. Siegenthaler and U. Eicher, in *Handbook of Holo-*

*cene Palaeoecology and Palaeohydrology*, B. E. Berglund, Ed. (Wiley, Toronto, 1986), pp. 407–422.
20. R. B. Alley *et al.*, *Geology* **25**, 483 (1997); J. Chappellaz *et al.*, *Nature* **366**, 443 (1993); P. A. Mayewski *et al.*, *Science* **263**, 1747 (1994).
21. K. A. Hughen, J. T. Overpeck, L. C. Peterson, S. Trumbore, *Nature* **380**, 51 (1996); J. C. Stager and P. A. Mayewski, *Science* **276**, 1834 (1997); U. von Grafenstein, H. Erlenkeuser, J. Muller, J. Jouzel, S. Johnsen, *Clim. Dyn.* **14**, 73 (1998).
22. G. Bond *et al.*, *Science* **278**, 1257 (1997).
23. Z. C. Yu, J. H. McAndrews, U. Eicher, *Geology* **25**, 251 (1997).

24. We thank J. Denhart, J. N. Haas, S. Hick, R. L. Jefferies, J. H. McAndrews, W. McKenna, L. C. K. Shane, and L. J. Wang for field, laboratory, and general assistance, and L. C. Cwynar, E. Ito, K. Kelts, J. H. McAndrews, D. M. Peteet, L. C. K. Shane, T. Webb III, and H. E. Wright Jr. for discussion and comments. Supported by the Natural Sciences and Engineering Research Council of Canada, Royal Ontario Museum, Ontario Ministry of Education and Training (Ontario Graduate Scholarship), and University of Toronto (Open Fellowships and Department of Botany).

28 April 1998; accepted 13 November 1998

# The Percolation Phase Transition in Sea Ice

**K. M. Golden,* S. F. Ackley, V. I. Lytle**

Sea ice exhibits a marked transition in its fluid transport properties at a critical brine volume fraction $p_c$ of about 5 percent, or temperature $T_c$ of about −5°C for salinity of 5 parts per thousand. For temperatures warmer than $T_c$, brine carrying heat and nutrients can move through the ice, whereas for colder temperatures the ice is impermeable. This transition plays a key role in the geophysics, biology, and remote sensing of sea ice. Percolation theory can be used to understand this critical behavior of transport in sea ice. The similarity of sea ice microstructure to compressed powders is used to theoretically predict $p_c$ of about 5 percent.

Sea ice is a complex, composite material consisting of pure ice with brine and air inclusions, whose size and geometry depend on the ice crystal structure, as well as the temperature and bulk salinity. It is distinguished from many other porous composites, such as sandstones or bone, in that its microstructure and bulk material properties vary dramatically over a small temperature range. For brine volume fractions $p$ below a critical value $p_c \approx 5\%$, columnar sea ice is effectively impermeable to fluid transport, whereas for $p$ above $p_c$ (>5%), brine or sea water can move through the ice. The relation of brine volume to temperature $T$ and salinity $S$ (*1*) implies $p_c$ corresponds to a critical temperature $T_c \approx -5$°C for $S = 5$ ppt; we refer to this critical behavior as the "law of fives." Perhaps the most direct observations of this are that the time rate of change of sea ice salinity $dS/dt$ due to gravity drainage vanishes for brine volumes below 5% (*2, 3*) and that the permeability of thin sea ice decreases by more than two orders of magnitude as the surface temperature is lowered, in a small critical region around −5°C (*4*).

Brine transport is fundamental to such processes as sea ice production through freezing of flooded ice surfaces, sea ice heat fluxes, and nutrient replenishment for sea ice algal communities, as well as being an important factor for remote sensing. However, the basic transition controlling brine transport has received little attention. Percolation theory (*5, 6*) has been developed to analyze the properties of materials where connectedness of a given component determines the bulk behavior. We show that it provides a natural framework to understand the critical behavior of sea ice. In particular, we apply a compressed powder percolation model to sea ice microstructure that explains the law of fives, the observed behavior (*4*) of the fluid permeability in the critical temperature regime, as well as data on surface flooding collected recently on sea ice in the Weddell Sea and East Antarctic regions.

It was observed in the Arctic (*7*) that a snow storm and its resultant loading on a sea ice layer can induce a complete upward flushing of the brine network. In the Antarctic, it was observed that the freezing of a surface slush layer, with resultant brine drainage, induced convection within the ice, whereby rejected dense brine is replaced by nutrient-rich sea water from the upper ocean (*8*), fueling autumn blooms of algae in second-year ice (*9*). During the autumn freeze-up, this process provided about 70% of the salt flux into the upper ocean and increased the total heat flux through the overlying ice and snow cover. The proliferation and growth of sea ice organisms is favored by permeable ice, which allows nutrient replenishment (*10, 11*). For remote sensing, surface flooding and subsequent freezing can affect microwave backscatter from sea ice (*12, 13*), and connectedness of the brine inclusions affects the permittivity of sea ice (*14, 15*). As yet another example, it was observed in the Arctic that there was about a 20-day time lag between the start of the spring snow melt and the occurrence of freshwater input into the mixed layer (*16, 17*). Presumably, part of this lag was the time it took for the ice sheet to warm to above the critical temperature to allow drainage out of the ice (*16*).

Percolation theory (*5, 6*) has been used to successfully model a broad array of disordered materials and processes. The simplest form of the lattice percolation model (*6*) is defined as follows. Consider the $d$-dimensional integer lattice $Z^d$ and the square (or cubic) network of bonds joining nearest neighbor lattice sites. To each bond, with probability $p$, $0 \le p \le 1$, we assign a 1, meaning it is open, and with probability $1 - p$ we assign a 0, meaning it is closed. Groups of connected open bonds are called open clusters, and the size of a cluster is just the number of open bonds it contains. In the percolation model, there is a critical probability $p_c$, $0 < p_c < 1$, called the percolation threshold, at which the average cluster size $\chi(p)$ diverges and an infinite cluster appears, so that the open bonds percolate. In two dimensions, $p_c = 0.5$; in three dimensions, $p_c \approx 0.25$. For $p > p_c$, the infinite cluster density $P_\infty(p)$ exhibits power law behavior near the threshold, $P_\infty(p) \sim (p - p_c)^\beta$, where $\beta$ is the percolation critical exponent, $\beta \le 1$. This model deals only with the geometrical aspects of connectedness in disordered media, yet we are interested in the transport properties as well. Then we consider a random resistor network, where the bonds are assigned the conductivities 1 and $h \ge 0$ with probabilities $p$ and $1 - p$. With $h = 0$, for $p < p_c$, the effective conductivity $\sigma(p) = 0$, whereas near the threshold with $p > p_c$, $\sigma(p)$ exhibits power law behavior $\sigma(p) \sim (p - p_c)^t$, where $t$ is the conductivity critical exponent, with $1 \le t \le 2$ in $d = 2,3$ (*18*). Analogously, we may consider a random pipe network with effective fluid permeability $\kappa(p)$ exhibiting similar behavior $\kappa(p) \sim (p - p_c)^e$, where $e$ is the permeability critical exponent, with $e = t$. Critical exponents for lattice models are generally believed to exhibit universality, meaning that they depend only on dimension and not on the type of lattice, although continuum models can exhibit nonuniversal behavior, with exponent values different from the lattice case, $t > 2$ in $d = 3$, and $e \ne t$.

If the above lattice model is applied to sea ice, where the open bonds represent brine and the closed bonds represent ice, then $p_c$ would be about 25% in $d = 3$, which is much larger than the observed 5%. Even continuum models, such as ellipsoidal brine inclusions randomly distributed in an ice host (a commonly used model for sea ice), exhibit critical volume fractions in the 20 to 40% range (*19*). Instead,

K. M. Golden, Department of Mathematics, University of Utah, Salt Lake City, UT 84112, USA. S. F. Ackley, U.S. Army Cold Regions Research and Engineering Laboratory, Hanover, NH 03755, USA. V. I. Lytle, Antarctic Cooperative Research Centre and Australian Antarctic Division, University of Tasmania, Hobart, Tasmania 7001, Australia.

*To whom correspondence should be addressed. E-mail: golden@math.utah.edu